ISSN: 2978-0632

*Review Article*

Open Access Journal of Physics and Science

# Establishment of an Application for Recognizing the Maturity of Cigar Leaf Using RGB Images

**Shuhua Zeng[1], Hao Yang[1], Weili Yang[2], Tong Zhang[1], Xiaoli Liu[1], Hongqi Zhang[1], Lei Liu[1], Xingyou Yang[3], Yajie Liu[1*], Shiping Guo[3*] and Huan Xiang[4*]**

[1]*College of Agriculture, Sichuan Agricultural University, Chengdu, Sichuan Province, 611130, China*

[2]*China National Tobacco Corporation Dazhou Tobacco Monopoly Bureau, Dazhou, Sichuan Province, 635000, China*

[3]*China National Tobacco Corporation Sichuan Branch, Chengdu, Sichuan Province, 610017, China*

[4]*Deyang Tobacco Monopoly Bureau of China National Tobacco Corporation, Deyang, Sichuan Province, 618400, China*

**[*]Corresponding authors**

Yajie Liu, College of Agriculture, Sichuan Agricultural University, Chengdu, Sichuan Province, 611130, China.

Shiping Guo, China National Tobacco Corporation Sichuan Branch, Chengdu, Sichuan Province, 610017, China.

Huan Xiang, Deyang Tobacco Monopoly Bureau of China National Tobacco Corporation, Deyang, Sichuan Province, 618400, China

**Received:** April 18, 2025; **Accepted:** April 22, 2025; **Published:** April 29, 2025

**Abstract**

To achieve objective and accurate recognition of the maturity of cigar leaves, industrial cameras were used to capture images of cigar leaves at three different maturity levels of cigar leaves: immature, mature, and overripe. MATLAB was used to establish the AlexNet and ResNet_18 classification models. The results showed that both ResNet_18 and AlexNet achieved higher accuracy during the training process with optimized structure 2 than with the classical structure and optimized structure 1. InitialLearnRate and MiniBatchSize achieved the highest accuracies of 0.001 and 32%, respectively. The precision, recall, and F1 score of ResNet_18 after the improvement were higher than those of AlexNet, with increases of 1.7%, 3.3%, and 0.026, respectively. The model generalization test showed ideal results, with an average accuracy of over 79% for both varieties and a discrimination accuracy of 92% for the unripe variety Chuanxue 1. The developed application can quickly and accurately identify the maturity of cigar leaves, thereby providing a method for determining maturity.

**Keywords:** Cigar Leaf, Maturity, Model, Identifying Applications

## Introduction

Maturity is the mature state exhibited by cigar leaves during their growth and development in the field and is also a core factor in the formation of tobacco quality [1]. Accurate discrimination of the maturity of fresh cigar leaves in the field is vital to ensuring tobacco quality. Currently, the maturity of cigar leaves is often judged visually based on the number of days after transplantation and leaf color [2,3]. Compared to flue-cured tobacco leaves, cigar leaves have more minor differences in leaf color in different parts, and visual discrimination is easily affected by the environment, resulting in subjective discrimination with intense subjectivity and significant errors [4-6].

The rapid development of machine vision technology in recent years has been widely applied in agriculture, medicine, and engineering [7-10]. Machine vision combines image processing and machine learning, providing a method for scientifically discriminating tobacco maturity. Many previous studies on the recognition of tobacco maturity have achieved ideal results. Li Yunjie et al. [11] collected images of tobacco with different maturity levels and constructed a tobacco maturity recognition model using the XGBoost algorithm, Du Pengcheng, Wang Ruiqi, and others have established a tobacco maturity recognition method based on the YOLO v5s algorithm for tobacco images [12,13], Lu Zhenshan [14] established a maturity recognition program for tobacco based on ResNet. Many studies have used images to distinguish the maturity of tobacco, however, little research has been conducted on cigar leaves. However, there were significant differences between the cigar leaves and flue-cured tobacco leaves regarding variety and cultivation methods.

**Citation:** Shuhua Zeng, Hao Yang, Weili Yang, Tong Zhang, Xiaoli Liu, et al. Establishment of an Application for Recognizing the Maturity of Cigar Leaf Using RGB Images. Open Access J Phys Sci. 2025. 2(2): 1-8. DOI: doi.org/10.61440/OAJPS.2025.v2.08

Given this, this study sets different harvesting maturity treatments to obtain RGB images of cigar leaves with different maturity levels and establishes an image-based application for cigar tobacco maturity discrimination to provide a method for intelligent recognition of tobacco maturity.

## Materials and Methods

### Test Site and Materials

The experiment was conducted in Sujiaqiao Village, Shifang City, Deyang City, Sichuan Province (31.20° N, 104.08° W), and Yantan Village, Fengcheng Town, Dazhou City, Sichuan Province (31.54° N, 108.01° W). The experimental varieties used were Dexue 1 and Chuanxue 1. The cigar leaf image acquisition device was a low-cost industrial camera sensor (model MVL-MF0828M-8MP).

### Experimental Design

Central cigar leaves ($9^{th}$ to $12^{th}$ leaf positions from bottom to top) were selected as the experimental subjects, and three maturity levels were set for the treatment: immature, mature, and over-ripe. The plant spacing and row spacing of the planting land in Shifang are 0.38 m and 1.1 m, respectively, while the planting land in Dazhou is 0.4 m and 1.1 m, respectively. Field measures, such as land preparation, ridge formation, fertilization, and transplanting, were uniformly managed with precision and carried out according to the cultivation techniques of eggplant clothing in Shifang and Dazhou. The nitrogen application rate in Shifang is 142.5 kg/hm$^2$, N: P2O5: K2O is 1:1.2:2.4, Dazhou is 202.5 kg/hm$^2$, and N: P2O5: K2O is 1:1.1:2.

### Image Acquisition of Tobacco Leaves

After each processed cigar leaf was harvested, it was immediately photographed to obtain images. The shooting environment is shown in Figure 1, with black baffles on the top, bottom, left, right, and back, and 1/3 of the front panel on the left for the easy retrieval and placement of cigar leaves. Equipped with filled lights on the top, left, and right, cigar leaves were placed at the bottom, and the camera was connected to an external computer.

**Figure 1:** Cigar Leaf Shooting Device

### Selection of Discriminant Models

ResNet-18 and AlexNet, two classic deep convolutional neural networks with 71 and 25 layers, respectively, were selected as the classification models for this experiment. The model-building framework was the deep-learning toolbox in MATLAB. The structure, optimizer, and hyperparameters of the two models were adjusted and compared, and the classification effect of the models with different layers on the different maturity levels of eggplant tobacco leaves was explored. The required image pixels for the model were 224 × 224 × 3 and 227 × 227 × 3, whereas the original image pixels were 4864 x 2498 x 3. It is necessary to adjust the original image pixels to satisfy the requirements of the model.

### Optimizer Selection

The function of the optimizer is to adjust the model's loss function, help the model gradually approach the optimal solution, and improve its classification capability. Standard optimizers include Stochastic Gradient Recent Momentum (Sgdm), Root Mean Square Prop (Rmsprop), and Adaptive Moment Estimation (Adam). Both models used Sgam as an optimizer.

### Research on Hyperparameters

For deep convolutional neural networks, the initial learning rate and minibatch size are the two hyperparameters most affecting model convergence and loss reduction. InitialLearnRate guides the network weights' hyperparameters by adjusting the network loss function's gradient, representing the information accumulation speed over the training time. When the learning rate is optimal, the adequate capacity of the model is maximized. The larger the InitialLearnRate, the greater the output error, and the more significant the impact of abnormal data, The smaller the InitialLearnRate, the slower and more complex the network convergence speed. Minibatch Size represents the number of samples selected for a single training session in a network. With a default training cycle of 1, if there are 10000 samples and the MiniBatchSize is 20, the number of samples trained in one session is 500. Usually, the larger the MiniBatchSize, the stronger the computational power of the matrix multiplication and the better the training effect of the network. However, the larger the GPU memory consumption, the lower the MiniBatchSize will generate more noise in the error calculation process. This experiment set different InitialLearnRate and MiniBatchSize sizes to determine the optimal combination.

### Model Evaluation Methods

The training process and generalization ability testing of AlexNet and ResNet_18 are evaluated using accuracy metrics, and the specific calculation formula is:

$$Accuracy(\%) = \frac{Pr}{TR}$$

where $Pr$ represents the number of correctly classified samples, and $Tr$ represents the total number of samples.

After determining the structure and hyperparameters, the model was evaluated using a confusion matrix, also known as an error matrix, a commonly used method for evaluating the accuracy of image classification models. The structure is shown in Figure 2, where the matrix rows represent the predicted values, and the list represents the true values. The confusion matrix statistics four types of indicators: When the true and predicted values are positive, they are called True Positive (TP), When the true value is positive and the predicted value is negative, it is called False Negative (FN), When both the true and predicted values are negative, it is called True Negative (TN), When the true

value is negative and the predicted value is true, it is called True Negative (TN).

| Confusion Matrix | | True Value | |
|---|---|---|---|
| | | Positive | Negative |
| Estimate Value | Positive | TP | FP |
| | Negative | FN | TN |

**Figure 2:** Confusion Matrix

The precision, recall, and F1 scores were calculated based on the confusion matrix. The accuracy is the proportion of model predictions for all positive results. The recall rate is the proportion of model predictions to all results, where the true value is positive. The F1 score combines the output of accuracy and recall and evaluates the entire model prediction. Its value is within [0,1], and the closer it is to 1, the better the model prediction. The calculation formulas are as follows:

$$Precision = \frac{TP}{TP+FP}$$

$$Recall = \frac{TP}{TP+FN}$$

$$F1\ Score = \frac{2\times Pr\times Re}{Pr+Re}$$

In the formula, Pr represents precision, and Re represents recall.

**Data Processing Methods**

MATLAB was used for model building and system construction. The MATLAB software, hardware experimental environment, and version information are presented in Table 1.

**Table 1: Software and Hardware Configuration Environment**

| Item | Configure Environment |
|---|---|
| processor | 12th Gen Inter(R) i5-12400f 2.50GHz |
| Running memory | 16GB |
| System disk | 500GB |
| operating system | Windows 10 |
| Deep learning framework | Matlab Neural Network Toolbox |
| programming language | Matlab 2023a |

**Results**

**Results of Tobacco Leaf Image Acquisition**

According to method 1.3, a total of 3043 images were collected for the two varieties in the 2022 experiment, as detailed in Table 2.

**Table 2: Results of Cigar Leaf Image Acquisition**

| Variety | Treatment | | | Total |
|---|---|---|---|---|
| | Immature | Mature | Overripe | |
| Dexue 1+Chuanxue 1 images | 1116 | 943 | 979 | 3043 |

**AlexNet Recognition Model Establishment**

**Convolutional Layer Design**

The input of AlexNet is the captured RGB color image, and the output is the name of each mature cigar leaf image folder. Precisely, before training, the images of each category are placed in different folders, named after the corresponding maturity category, specifically "immature," "mature," and "overripe." The classic AlexNet structure is built in the Deep Learning Toolbox app in MATLAB and AlexNet structures 1 and 2 are optimized by adjusting the number and size of the convolutional blocks. The results are summarized in Table 3. The images of the two varieties of cigar leaves are divided according to the 4:1 division rule, 80% of the samples for training and 20% for testing are randomly determined, and model training and testing is conducted.

**Table 3: Three Model Structures of AlexNet**

| Classic structure | Optimizing Structure 1 | Optimizing Structure 2 |
|---|---|---|
| Convolutional layer 1, [11×11, 96, [4 4]] | Convolutional layer 1, [11×11, 96, [4 4]] | Convolutional layer 1, [11×11, 96, [4 4]] |
| Convolutional layer 2, [5×5, 128, [1 1]], 2 groups | Convolutional layer 2, [5×5, 128, [1 1]], 2 groups | Convolutional layer 2, [5×5, 128, [1 1]], 2 groups |
| Convolutional layer 3, [3×3, 384, [1 1]] | Convolutional layer 3, [3×3, 384, [1 1]] | Convolutional layer 3, [3×3, 384, [1 1]] |
| Convolutional layer 4, [3×3, 192, [1 1]], two groups | Convolutional layer 4, [3×3, 192, [1 1]], two groups | Convolutional layer 4, [3×3, 192, [1 1]], two groups |
| Convolutional layer 5, [3×3, 128, [1 1]], two groups | Convolutional layer 5, [3×3, 128, [1 1]], two groups | |
| | Convolutional layer 6, [3×3, 324, [1 1]] | |

The discrimination accuracies of the three AlexNet structures for the test set samples are shown in Figure 3. AlexNet-optimized structure 2 exhibited the highest discrimination accuracy (93.6%). From the perspective of the entire training process of the model, the classical structure training process has a smaller oscillation amplitude and a smoother process. When optimizing structures 1 and 2 with an iteration period of 100 to 200, the accuracy fluctuates greatly, but ultimately improves. Compared to a single variety, the training iteration period of the merged image set was doubled, and the training time was long. In summary, the discrimination accuracy of AlexNet-optimized Structure 2 was better than that of optimized Structure 1 and the classical structure.

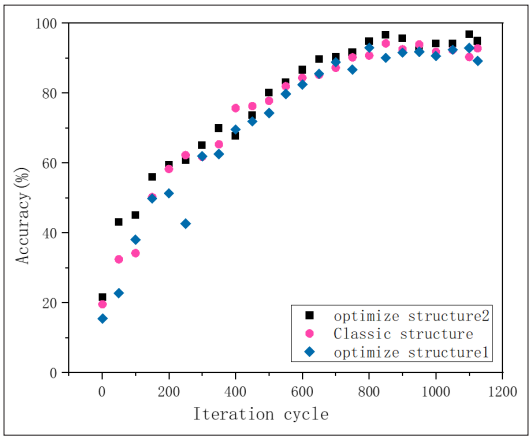


**Figure 3:** AlexNet Classic Structure, Optimized Structure 1, and Optimized Structure 2 Pairs Recognition accuracy of test set samples

### Research On Hyperparameters

#### Different MiniBatchSize

Comparative experiments were conducted using four sets of MiniBatchSizes: 16, 32, 64, and 128. The image sample partition rule is the same as that described in Section 3.9.1.1, and the test set results after training are shown in Figure 4. The discrimination effect was best when the MiniBatchSize was set to 32, with an accuracy of 93.5%. For AlexNet, setting the MiniBatchSize to 32 resulted in the best discrimination accuracy.

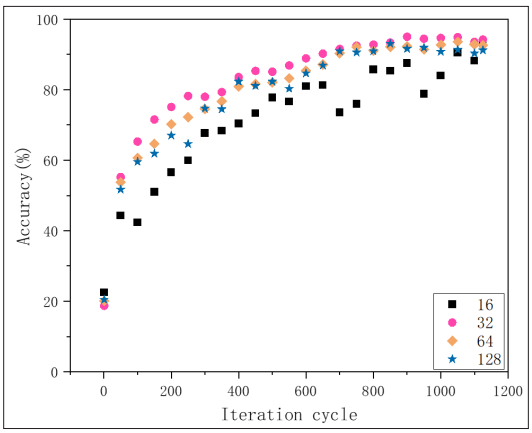


**Figure 4:** Discrimination accuracy of AlexNet with different MiniBatchSizes on the test set

#### Different Initial Learnrates

The discriminative effect of AlexNet was investigated by setting three learning rates (0.001, 0.0001, and 0.00001). The image sample partition rule is the same as that described in Section 3.9.1.1, and the test set results after training are shown in Figure 5. It can be seen that the highest discrimination accuracy is achieved at 0.001, with a discrimination accuracy of 92.7%. Therefore, the optimal learning rate for AlexNet is determined to be 0.001.

### Establishment of Improved AlexNet Model

The experimental results of Sections 2.2.1 and 2.2.2 determined that the recognition performance of AlexNet-optimized Structure 2 was better than that of optimized Structure 1 and the classical structure. The accuracy when iniBatchSize was set to 32 was significantly higher than when iniBatchSize was set to 16, 64, or 128. When InitialLearnRate was set to 0.001, the model stability and accuracy were higher than 0.0001 and 0.00001, respectively. An improved AlexNet model was established with optimized structure 2, iniBatchSize set to 32, and InitialLearnRate set to 0.001. The results are shown in Figure 6. It can be seen that only four samples of immature categories were misclassified, nine samples of mature categories were misclassified, and there was a higher number of misclassifications in overripe categories, at 12.

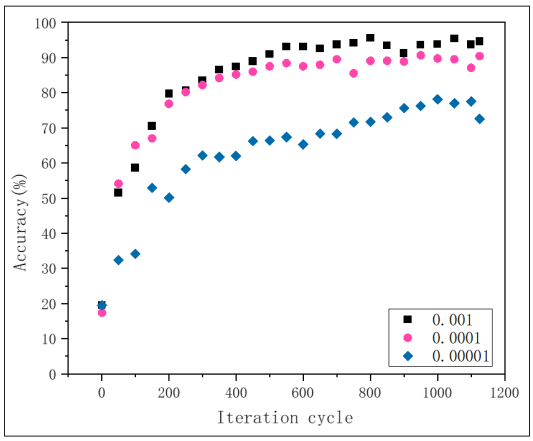


**Figure 5:** Discrimination accuracy of AlexNet for two image sets with different InitialLearnRates

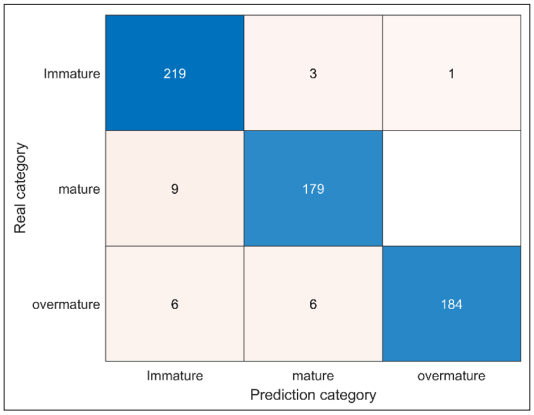


**Figure 6:** Improved AlexNet test set confusion matrix diagram

The accuracy, recall, and F1 score were calculated to be 1.6, as shown in Table 4. It can be seen that the overall precision of the model is 96.1, the recall rate is 94.4, and the F1 score is 0.952.

**Table 4: Precision, Recall, And F1 Score of The Improved AlexNet Test Set**

| Index | Training frequency | | | Average |
|---|---|---|---|---|
| | 1–10 | 11–20 | 21–30 | |
| Precision (%) | 98.2 | 95.2 | 94.9 | 96.1 |
| Recall (%) | 93.6 | 95.2 | 94.5 | 94.4 |
| F1 Score | 0.958 | 0.952 | 0.947 | 0.952 |

### ResNet-18 Other Methods

#### Convolutional Layer Design

The construction, folder naming, and sample partitioning rules for the different structures of ResNet_18 are the same as those in Section 2.2.1. The residual blocks of the ResNet_18 classical structure, optimized Structure 1, and optimized Structure 2 are listed in Table 5.

**Table 5: Three Model Structures of ResNet-18**

| Classic structure | Optimizing Structure 1 | Optimizing Structure 2 |
|---|---|---|
| Convolutional layer 1, [7×7, 64, [2 2]] | Convolutional layer 1, [7×7, 32, [2 2]] | Convolutional layer 1, [7×7, 64, [2 2]] |
| Residual block 2, $\begin{bmatrix}3\times3, & 64, & [1\ 1]\\ 3\times3, & 64, & [1\ 1]\end{bmatrix}\times2$ groups | Residual block 2, $\begin{bmatrix}3\times3, & 32, & [1\ 1]\\ 3\times3, & 32, & [1\ 1]\end{bmatrix}\times2$ groups | Residual block 2, $\begin{bmatrix}3\times3, & 64, & [1\ 1]\\ 3\times3, & 64, & [1\ 1]\end{bmatrix}\times2$ groups |
| Residual block 3, $\begin{bmatrix}3\times3, & 128, & [1\ 1]\\ 3\times3, & 128, & [1\ 1]\end{bmatrix}\times2$ groups, Branches, $[1\times1,\ 128]$,[2] | Residual block 3, $\begin{bmatrix}3\times3, & 64, & [2\ 2]\\ 3\times3, & 64, & [1\ 1]\\ 3\times3, & 64, & [1\ 1]\\ 3\times3, & 64, & [1\ 1]\end{bmatrix}$, branch, $[3\times3,\ 64,\ [1\ 1]]$ | Residual block 3, $\begin{bmatrix}3\times3, & 128, & [2\ 2]\\ 3\times3, & 128, & [1\ 1]\\ 3\times3, & 128, & [1\ 1]\\ 3\times3, & 128, & [1\ 1]\end{bmatrix}$, branch, $[1\times1,\ 128,\ [2\ 2]]$ |
| Residual block 4, $\begin{bmatrix}3\times3, & 256, & [1\ 1]\\ 3\times3, & 256, & [1\ 1]\end{bmatrix}\times2$ groups, Branches, $[1\times1,\ 256]$,[2] | Residual block 4, $\begin{bmatrix}3\times3, & 128, & [2\ 2]\\ 3\times3, & 128, & [1\ 1]\\ 3\times3, & 128, & [1\ 1]\\ 3\times3, & 128, & [1\ 1]\end{bmatrix}$, branch, $[1\times1,\ 128,\ [2\ 2]]$ | Residual block 4, $\begin{bmatrix}3\times3, & 256, & [2\ 2]\\ 3\times3, & 256, & [1\ 1]\\ 3\times3, & 256, & [1\ 1]\\ 3\times3, & 128, & [1\ 1]\end{bmatrix}$, branch, $[1\times1,\ 256,\ [2]]$ |
| Residual block 5, $\begin{bmatrix}3\times3, & 512, & [1\ 1]\\ 3\times3, & 512 & [1\ 1]\end{bmatrix}\times2$ groups, Branches, $[1\times1,\ 512]$,[2] | Residual block 5, $\begin{bmatrix}3\times3, & 256, & [2\ 2]\\ 3\times3, & 256, & [1\ 1]\\ 3\times3, & 256, & [1\ 1]\\ 3\times3, & 128, & [1\ 1]\end{bmatrix}$, branch, $[1\times1,\ 256,\ [2]]$ | |
| | Residual block 6, $\begin{bmatrix}3\times3, & 512, & [2\ 2]\\ 3\times3, & 512, & [1\ 1]\\ 3\times3, & 512, & [1\ 1]\\ 3\times3, & 512, & [1\ 1]\end{bmatrix}$ | |

As shown in Figure 7, there were differences in the discrimination of ResNet_18 with different structures in the image set. The differences during the training process of the classical structure, optimized Structure 1, and optimized Structure 2 were relatively small, with values of 97.4%, 97.9%, and 98.2%, respectively.

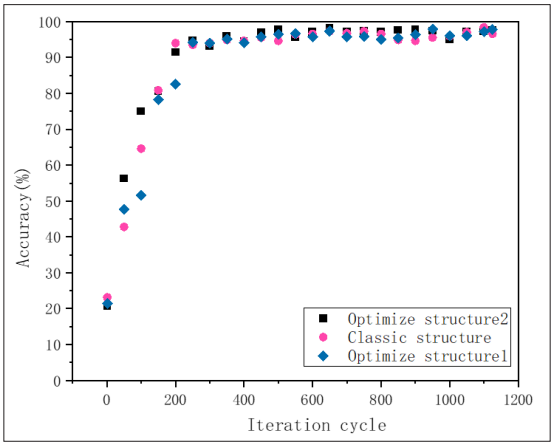


**Figure 7:** Accuracy of the Training Process for ResNet_18 With Different Structures

**Research on Hyperparameters**

**(1) Different MiniBatchSizes**

According to the image segmentation rules described in Section 2.2.1, comparative experiments were conducted using different MiniBatchSizes. The accuracy of the training process on the test set is shown in Figure 8, which indicates differences in the accuracy. Overall, the accuracy decreased with an increase in MiniBatchSize. During the entire training process, when the MiniBatchSize was 128 and 64, the oscillation amplitude of 50 to 150 iteration cycles was small, but the final accuracy decreased. When the MiniBatchSize was 16, the oscillation amplitude was larger, followed by 32. Compared to setting the MiniBatchSize to 16, setting it to 32 resulted in smaller oscillations and higher accuracy. Therefore, when the MiniBatchSize was set to 32, ResNet_18 performed the best.

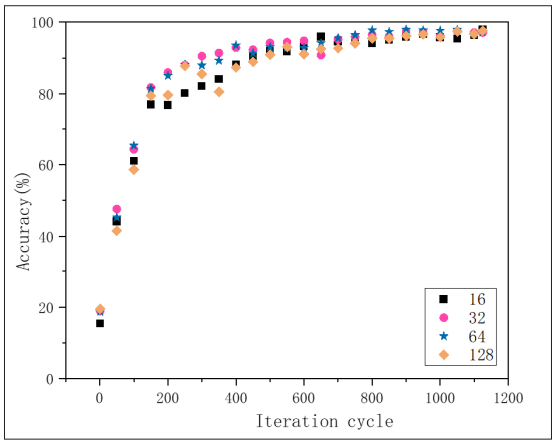


**Figure 8:** Accuracy of ResNet_18 Training Process for Different MiniBatchSizes

**(2) Different InitialLearnRate**

According to Partition Rule 2.2.1, comparative experiments are conducted for different InitialLearnRate sizes. The accuracy of the training process for the test set is shown in Figure 9. It can be seen that there is a significant difference in accuracy, with 0.001 having the best accuracy, followed by 0.0001, which has the lowest accuracy. From the training oscillation amplitude perspective, when InitialLearnRate was 0.00001, the oscillation was the largest, followed by 0.0001, and 0.001 had the smallest oscillation. Therefore, 0.001 was determined to be the optimal learning rate for ResNet_18.

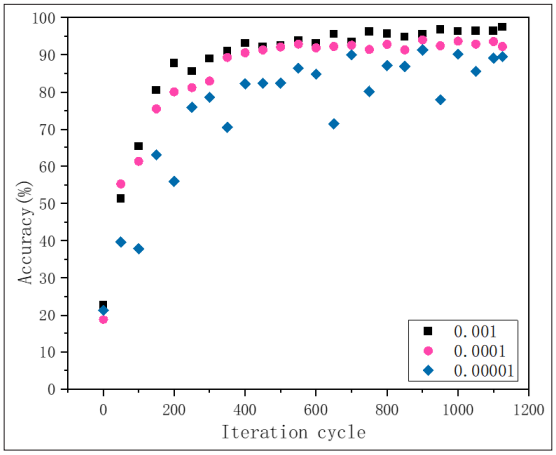


**Figure 9:** Accuracy of ResNet_18 Training Process for Different InitialLearnRates

**Improved ResNet_18 Model Establishment**

Based on the experimental results in Section 2.3.1 and 2.3.2, it was determined that the recognition performance of ResNet_18 optimized Structure 2 was better than that of optimized Structure 1 and the classical structure. The accuracy when iniBatchSize was set to 32 was significantly higher than when iniBatchSize was set to 16, 64, or 128. When InitialLearnRate was set to 0.001, the model stability and accuracy were higher than 0.0001 and 0.00001, respectively. An improved ResNet_18 model with an optimized structure 2, iniBatchSize set to 32, and InitialLearnRate set to 0.001. The results are shown in Figure 10. It can be seen that only eight samples of immature categories were misclassified, two samples of mature categories were misclassified, and four samples of overripe categories were misclassified.

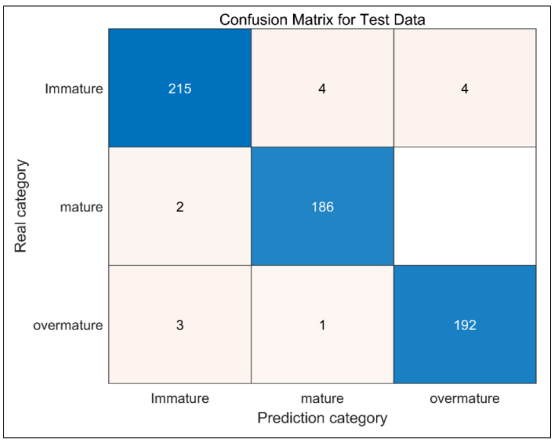


**Figure 10:** Improved Resnet_18 Test Set Confusion Matrix Diagram

The precision, recall, and F1 scores were calculated as 1.6, as shown in Table 6. It can be seen that the overall precision of the model is 97.8%, the recall rate is 97.7%, and the F1 score is 0.978. After 30 rounds of model training, the ideal effect was still achieved, indicating the strong stability of the model.

**Table 6: Precision, Recall, and F1 Score of the Improved ResNet_18 Test Set**

| Index | Training frequency | | | Average |
|---|---|---|---|---|
| | 1–10 | 11–20 | 21–30 | |
| Precision (%) | 96.4 | 98.9 | 98.0 | 97.8 |
| Recall (%) | 97.7 | 97.4 | 98.0 | 97.7 |
| F1 Score | 0.972 | 0.981 | 0.980 | 0.978 |

Model Generalization Ability Testing

Based on the experimental results of 2.2.3 and 2.3.3, it was determined that the precision, recall, and F1 score of the improved ResNet_18 are higher than AlexNet by 1.7%, 3.3%, and 0.026%, respectively. Generalization testing was performed using the improved ResNet_18 model. Generalization ability is an important step in testing whether a model overfits. The test tobacco leaf was a cigar tobacco leaf image taken in 2023 using the same shooting method described in Section 2.5.1. The number of tests was 50, with randomly selected samples from each variety and maturity level, and the test results are shown in Table 7. The table shows that the constructed model has a good classification effect on the generalization test samples, with an average accuracy of over 79% for both varieties and a discrimination accuracy of 92% for immature Chuanxue 1.

**Table 7: The Generalization Test Results of the Build Model**

| Treatment | | Test samples | Properly classify samples | Accuracy (%) | Average of accuracy (%) |
|---|---|---|---|---|---|
| | immature | 50 | 45 | 90.0 | |
| Dexue 1 | mature | 50 | 35 | 70.0 | 79.3 |
| | overripe | 50 | 39 | 78.0 | |
| | immature | 50 | 46 | 92.0 | |
| Chuanxue 1 | mature | 50 | 38 | 76.0 | 85.3 |
| | overripe | 50 | 44 | 88.0 | |

**Maturity Recognition Application (APP) Construction**

**Practical Analysis of APP**

Practicality analysis analyzes the functionality, interface layout, usage efficiency, and other aspects of building an app to plan for future actions. The APP's primary function is to achieve rapid and accurate recognition of the maturity of cigar leaves, overcoming the intense subjectivity of manual recognition. In addition, the APP can provide a recognition platform for users interested in recognizing cigar leaf maturity. The functions to be implemented by the APP can be divided into three operational steps:

**(1) Image upload**

To solve the problem of different image formats captured by different devices, the APP must be able to import images in all formats, such as JPG, BMP, PNG, and JPEG.

**(2) Image maturity discrimination**

This function must achieve the maturity discrimination of the uploaded images through the constructed classification model. Therefore, this step requires implementing a callback classification model for image maturity discrimination.

**(3) Display of discrimination results**

The discrimination results were divided into three maturity levels: immature, mature, and overripe. Therefore, this step primarily displays the classification results for the main interface. Based on the results of this study, corresponding suggestions should be made regarding the results identified in this step. The rules are as follows: when the identified result is immature, it is recommended to delay the harvest owing to insufficient maturity of the cigar leaves, when the discrimination result is mature, it is recommended to harvest the cigar leaves immediately if their maturity is appropriate, when the result is overripening, the cigar leaves have a higher maturity, and it is recommended to harvest them immediately.

**APP Building Methods**

The APP building environment is a Matlab APP design tool with the same software and hardware information as described in Section 2.6.

**(1) Implementation of image upload function**

[file, path] =uigetfile ({'*. jpg, *. png, *. jpeg', 'Image Files (*. jpg, *. png, *. jpeg)'}), which allows for the selection of

all image formats. Image=imread (full file (path, file)) opens the image in the device image. Imshow (image, 'Parent', app. UIAxes) displays an imported image on the app interface. App I=image and implement callback for the entire APP.

**(2) Implementation of classification function**

I2=immesize (app. I, [224224]) to achieve image size compression. Da=load ("trainedNetwork. mat", 'net') implements the deep network model built by callback. [preLabels, probis] =classify (net, I2), the classification function is implemented by calling the model.

**(3) Display of the classification results**

App EditField Value=char (preLabels) and app TextArea Value=aa (nn) display the classification results and corresponding suggestions for the interface, respectively.

**APP Operation**

After completing the APP design using Matlab design tools, it was packaged and installed in Malab to construct the entire APP. The established APP in the MATLAB APP tab and clicked to enter the system, as shown in Figure 11. The next step was to select an image for maturity discrimination.

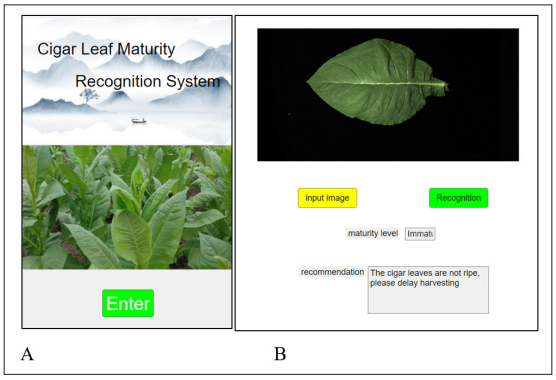


**Figure 11:** APP Runs into System Interface (A) and Classification Interface (B)

**Discussion**

Objectively and accurately determining the maturity of cigar leaves is a key step toward improving the quality of blended cigar leaves. Machine vision technology can accurately capture color differences in the appearance of cigar leaves and reflect their maturity. There is extensive research on discriminating the maturity of cigar leaf harvests in the field. For example, Wang Jie et al. [15] constructed an ELM to classify flue-cured tobacco, and its test set accuracy reached 96.43%, Liang Yin[16] and Li Xin[17] established an SVM flue-cured tobacco maturity classification model based on hyperspectral information, and the accuracy of the test set was above 90%, Chang Jianwei et al. established a BPNN for determining the maturity of flue-cured tobacco, with a test set accuracy rate of 90%, Zhang Chunchun et al.[18] used transfer learning methods to perform microstrip green flue-cured tobacco leaf recognition on the fine-tuning MobileNet model, and the recognition accuracy reached 100%. It can be seen that the recognition of flue-cured tobacco leaves is currently relatively mature. In determining the maturity of cigar harvesting, Wang Dabin et al. [19] established an SVM by collecting hyperspectral information to classify the harvest maturity of CX-80 cigar leaves with a classification accuracy of 98%. Yao Heng et al. [20] invented a SPAD-based method for determining the maturity of cigar leaves. This study established ResNet_18 and AlexNet classification model using RGB images captured by industrial cameras and compared the structure and hyperparameters of these model. The results indicate that ResNet_18 and AlexNet had better classification performance, and both models achieved higher recognition accuracy in the optimized structure 2 test set compared to the classical structure and optimized structure 1. The results of hyperparameter research indicate that the model recognition accuracy is highest when the MiniBatchSize and InitialLearnRate of ResNet_18 and AlexNet are 32 and 0.001, respectively. Compared to the classical structure and optimized structure 1, optimized structure 2 reduces the number of convolutional layers. Theoretically, the reduction in convolutional blocks reduces the depth of the extracted features, however, this study improved the classification accuracy. This may be because the image elements captured in this experiment were relatively single (cigar leaves), and fewer convolutional layers and residual blocks were suitable for this image set. After the model is established, it is usually necessary to establish recognition mini-programs or application software to achieve a practical application of the model. This study successfully designed the established model as a recognition application. In future applications, the cigar leaf image will be uploaded to a computer to achieve recognition of the new image.

**Conclusions**

This study collected images of cigar leaves at different maturity levels to distinguish the maturity, and the results were ideal. The following conclusions can be drawn: ResNet_18 and AlexNet both achieved higher accuracy in the training process of optimized structure 2 than in the classical structure and optimized structure 1, whereas InitialLearnRate and MiniBatchSize achieved the best accuracies at 0.001 and 32. The precision, recall, and F1 score of ResNet_18 after the improvement were higher than those of AlexNet, with increases of 1.7%, 3.3%, and 0.026, respectively. The model generalization test showed ideal results, with an average accuracy of over 79% for both varieties and a discrimination accuracy of 92% for the immature Chuanxue 1. The developed application can quickly and accurately identify the maturity of cigar leaves, thereby providing a method for determining maturity.

**Acknowledgements**

This work was partly supported by the Intelligence Agriculture Research Office Team, Sichuan Agricultural University.

**Author Contributions**

Shuhua Zeng and Hao Yang: writing and original editing, Weili Yang: provide cigar leaf resources, Tong Zhang, Xiaoli Liu and Hongqi Zhang: field investigation and image shooting, Shiping Guo, Huan Xiang and Yajie Liu: provide financial support, Lei Liu and Xingyou Yang: provide method support

**Funding Statement**

This work was supported by the Supported by China National Tobacco Corporation Sichuan Provincial Company (NO. SCYC202121)

**Competing Interests**

The authors declare that the research was conducted in the absence of any commercial or financial relationships that could be construed as a potential conflict of interest

**Ethical Standards**
Not Applicable

**Supplementary Explanation**
The images of cigar leaves in this experiment can be obtained through the Google Drive open link below

**Overmature:**
https://drive.google.com/drive/folders/1DXBXpntpgLMO5kueUjAK26XiI9HuzPru?usp=sharing

**Immature:**
https://drive.google.com/drive/folders/1R2cgRZQaEes4hG1BolKGpcH4mzuPzOzr?usp=sharing

**Mature:**
https://drive.google.com/drive/folders/1qt05kO0DL8-xP13TQnXguqXs334N3zcL?usp=sharing

**References**

1. Xu ZC, Zhao RR, Wang LX, Jiao JH, Song PF. Research Progress on Tobacco Maturity. Journal of Northeast Agricultural University. 2014. 45: 123-128.
2. Wang Q, Xi L, Reng YN, Ma XM. A Method for Determining Tobacco Maturity Based on Computer Vision Technology. Journal of Agricultural Engineering. 2012. 28: 175-179.
3. Jiang BC, Li DL, Wei KS, Zhang FG, Wang J, et al. (2022) A Study on the Estimation Model of Chlorophyll Content in Flue-Cured Tobacco Based on Hyperspectral. China Journal of Agricultural Machinery Chemistry. 2012. 43: 104-110.
4. Wan D, Yu YZ, Xu FS, Yu J, Qiao BM, et al. Characterization and Analysis of Maturity of Cigar Tobacco Leaves. Molecular plant breeding. 2022. 01-11.
5. Li YF. Research on physiological and biochemical mechanisms and maturation standards during the maturation process of high-quality cigar coat. Henan Agricultural University. 2019.
6. Jiang DL. Research on maturation characteristics and harvesting time of Hainan cigar coat. Henan Agricultural University. 2018.
7. Wen MQ, Reng LQ, Chen ZQ, Yang Z, Zhan YM. A Review of Deep Learning Based Line of Sight Estimation Methods. Computer Engineering and Applications. 2024. 05: 01-19.
8. Liu AW, Xie FP, Xiang Y, Li YJ, Lei XM. A Machine Vision Based Automatic Eye Removal Method and Experiment for Pineapple. Journal of Agricultural Engineering. 2024. 05: 01-10.
9. Huang XR, Huang HS, Huang YC, Chen MN, Fan XY, et al. The Application of Video Based Action Intelligent Recognition in Medicine. Chinese Journal of Medical Physics. 2024. 41: 01-07.
10. Mou XG, Wang WH, Zhao HL, Li FC, Liu C, et al. Development and Application of a Machine Vision Based Surface Defect Detection System for Aluminum Clad Steel Busbars. Shanghai Metal. 2024. 46: 89-94.
11. Li YJ, Chen ZG, Sun JG, Li JP, Feng J, et al. Image Recognition of Tobacco Harvest Maturity Based on XGBoost Algorithm. Chinese Journal of Tobacco. 2024. 31: 01-14.
12. Du PC, Jiang DZ, Xiang Y, Jing LH, Wu SG, et al. A method for identifying the maturity of fresh tobacco leaves based on YOLO v5s object detection algorithm. Jiangsu Agricultural Sciences. 2023. 51: 158-165.
13. Wang RQ, Zhang BH, Gu G, Shen SJ, Lin XL, et al. Research on the Maturity Recognition Model of Fresh Tobacco Leaves Based on YOLOv5. Chinese Journal of Tobacco. 2022. 29: 46-55.
14. Lu ZS. Research and application of tobacco maturity determination based on ResNet. Guilin University of Electronic Science and Technology. 2023.
15. Wang J, Bi HY Classification of Tobacco Maturity Based on Extreme Learning Machines. Tobacco Technology. 2013. 05: 17-19.
16. Liang Y, Zhang YW, Li JY. Hyperspectral Remote Sensing Recognition of Yunyan 87 Tobacco Leaf Maturity Based on Support Vector Machine. Southwest Agricultural Journal. 2013. 26: 957-962.
17. Li X, Tang WR, Zhang YH, Xie Q, Zhang F, et al. A maturity discrimination model for tobacco leaves in the field based on hyperspectral imaging technology. Tobacco Technology. 2022. 55: 17-24.
18. Zhang CJ, Luo RL, Lu L, Chen ZQ, Yun LJ. Microstrip Green Tobacco Leaf Image Recognition Based on MobileNet and Transfer Learning. Journal of Yunnan Normal University. Natural Science Edition. 2023. 43: 46-48.
19. Wang DB, Meng GX, Wang XS, Chen HH, Deng JQ, et al. Analysis of Hyperspectral Characteristics and Construction of Classification Models for Tobacco Leaves with Different Maturity Levels of Eggplant Cover. Chinese Tobacco Science. 2023. 44: 85-91.
20. Yao H, Kong GH, Zhang GH, Zhao GK, Wu YP, et al. Method for judging the maturity period of cigar leaf harvesting based on SPAD difference. 2024. 202211456615.